Available online at www.sciencedirect.com

SciVerse ScienceDirect

Ceramics International 39 (2013) 819–827

CERAMICS INTERNATIONAL

www.elsevier.com/locate/ceramint

Facile synthesis of zinc carbonate and zinc oxide nanoparticles via direct carbonation and thermal decomposition

Mojtaba Shamsipur[a,*], Seied Mahdi Pourmortazavi[a,b,**], Seiedeh Somayyeh Hajimirsadeghi[c], Mir Mahdi Zahedi[c], Mehdi Rahimi-Nasrabadi[d]

[a]*Department of Chemistry, Razi University, Kermanshah, Iran*
[b]*Faculty of Material and Manufacturing Technologies, Malek Ashtar University of Technology, Tehran, Iran*
[c]*Islamic Azad University, Varamin Pishva Branch, Varamin, Iran*
[d]*Department of Chemistry, Imam Hossein University, Tehran, Iran*

Received 28 April 2012; received in revised form 28 June 2012; accepted 1 July 2012
Available online 10 July 2012

Abstract

Synthesis of ultrafine zinc carbonate and zinc oxide powders using direct precipitation and thermal decomposition of the precursor was investigated. Nanoparticles of $ZnCO_3$ were prepared by the direct precipitation method with $Zn(NO_3)_2$ and Na_2CO_3 as raw materials. The precipitation process as a popular, facile, controllable and cost-effective method was used to produce insoluble inorganic salts. Therefore, it was very important to improve capability and quality of the process for controlling the product particle size by setting the optimal precipitation reaction parameters. In this research, the parameter design of the Taguchi method was applied to set the optimal parameters of precipitation process for zinc carbonate nano-particle preparation. The reaction conditions such as zinc and carbonate ion concentrations, flow rate of reagent addition and reactor temperature were optimized by orthogonal array design, OA_9. The effect of these factors on the size of $ZnCO_3$ nanoparticles was quantitatively evaluated by the analysis of variance (ANOVA). The results showed that $ZnCO_3$ nanoparticles can be synthesized via direct carbonation process by controlling zinc and carbonate ion concentrations and flow rate of reagent addition. The experimental results for preparation of nano-particles of $ZnCO_3$ showed that the minimum size was about 15 nm and the maximum was about 70 nm. In the next step of this study, an efficient one-step thermal decomposition method was described for preparation of ZnO nanoparticles from zinc carbonate precursor. The prepared $ZnCO_3$ and ZnO particles were characterized using X-ray diffraction (XRD), SEM, FT-IR and thermal analysis techniques.

Keywords: Particle size control; Thermal decomposition; Zinc carbonate; Zinc oxide

1. Introduction

Recently, preparation of artificially designed structure of nanoparticles with new properties has attracted the attentions of many researchers [1,2]. Nanoparticles compounds with well-defined structures prepared from tailored nanoparticles provide opportunities for optimizing properties of materials and offer possibilities for observing interesting and potentially useful new properties [3–5]. Although, the fabrication of zinc carbonate nanostructures has not necessarily been directed to practical applications. But we believe that these nanostructures should be more precisely tailored in accordance with microstructural features required in each specific application, because zinc carbonate compound is used in respirators to remove toxic gases such as SO_2 and HCN [6,7]. Therefore, particle size reduction and hence increasing the specific surface area of zinc carbonate could affect strongly on the performance of repirators containg this compound. Also, zinc carbonate is an useful precursor for the preparation of zinc oxide particles [8–10]. Its means that preparation of zinc

*Corresponding author.
**Correspondence to: P.O. Box 16765-3454, Tehran, Iran. Fax: +98 212 2936578.
E-mail addresses: mshamsipur@yahoo.com (M. Shamsipur), pourmortazavi@yahoo.com (S.M. Pourmortazavi).

0272-8842/$36.00 © 2012 Elsevier Ltd and Techna Group S.r.l. All rights reserved.
http://dx.doi.org/10.1016/j.ceramint.2012.07.003

carbonate nano-sized precursor for synthesis of zinc oxide nanoparticles via a solid reaction is interested [11,12].

Until today, several synthesis methods are described for the preparation of zinc carbonate [13–16]. Zhang et al. [13] reported a method for preparation of zinc carbonate via hydrothermal synthesis from the reaction of $ZnCl_2$ and K_2CO_3. Feng et al. [14] also prepared $ZnCO_3$ via the micro-emulsion method, but the process was rigorous and it was not easy to prepare the product on a large scale. Wu and Jiang [15] synthesized nanocrystalline $ZnCO_3$ via solis-solid reaction by grinding $ZnSO_4 \cdot 7H_2O$ and NH_4HCO_3 with surfactant OP thoroughly at room temperature. Although, these methods proposed various techniques for preparation of zinc carbonate, but these techniques have their own limitations and disadvantages especially for large scale production of the product. Therefore, investigation for finding a facile and cost effective method for synthesis of nanoparticles of this compound is required, especially if the proposed technique has an appropriate potential for scaling up and production of the product in large scales.

Precipitation plays an important role in the field of bulk nanoparticle preparation [16,17]. High degree of flexibility of this method makes it possible to create pure materials with homogeneous distributions; therefore, it is one of the most frequently applied synthetic methods. In this technique the degree of supersaturation that is created by bringing the corresponding solutions into contact is essential for the particle formation [18]. During a conventional precipitation in a batch reactor local supersaturation is created when a droplet of one solution hits the other solution. Due to intensive stirring the system is homogenized on a short timescale, and the local supersaturation vanishes.

Calcination is the process of heating a solid material to drive off volatile chemically combined components, e.g., carbon dioxide [19–25]. Although various methods were used to prepare nanometer-sized zinc oxide [26–29], but the most promising one was thermal decomposition or calcinations of zinc carbonate and zinc carbonate hydroxide precursors. While, the raw materials for this process are easily available and have a low-cost, superfine ZnO product can be easily prepared by using this technique. Therefore, various techniques for synthesis of these precursors were widely studied, and the mechanism and kinetics of thermal decomposition of zinc carbonates and zinc carbonate hydroxides were reported by several authors [30–32]. It is clear that the calcination reaction for the preparation of a defined oxide product is a complex process depending on both the experimental conditions (surrounding environment, heating rate, reactant mass, and type of crucible) and the possibility of occurrence of secondary processes [33]. In this respect, the effect of the conditions for the preparation of the precursor on its properties and thermal stability should also be mentioned [34]. These are factors influencing substantially the properties of the oxide product obtained. On the other hand, it is known that by varying the concentration of the starting solutions and the crystallization procedure, a crystalline precipitate with differently developed surface area can be obtained, which defines the dispersity of the oxide product obtained. For this reason, it is quite important to set appropriate conditions for the precursor synthesis and to follow its decomposition by comparing different methods. This will elucidate the mechanism of formation of the final product and will provide a possibility of selection of reproducible conditions for the synthesis of an oxide product with desired properties depending on its application [35].

Ultrafine zinc oxide particles are attractive for solar energy conversion [36], non-linear optics [37], catalysis [38], and pigments [39]. ZnO nanoparticle is an important wide band gap semiconductor material, which has a potential for the application in many areas, such as UV light emitting diodes, UV laser, gas sensors, photo-catalysts, and photovoltaic devices [40–43]. Zinc oxide is also a kind of representative electrochemical and photochemical semiconductor [44–46]. Until today, various techniques have been employed to prepare ZnO nanoparticles, including sol–gel, hydrothermal synthesis, chemical vapor deposition, thermal oxidation, electrodeposition, etc. [47–49]. However, due to the high importance and wide application of ZnO nanaoparticles researches for synthesis of this compound with desired morphology via a cost effective method is under development.

This research aims at the preparation of $ZnCO_3$ nano-sized particles with high purity using the direct carbonation technique which is a facile and cost effective method; also it is capable of large scale production. Therefore, zinc carbonate nanoparticles with spherical morphology were prepared via the direct precipitation method by reaction between $Zn(NO_3)_2 \cdot 7H_2O$ and Na_2CO_3 in aqueous media. An experimental design procedure was used to investigate the effects of various experimental reaction parameters on the particle size of zinc carbonate formed, i.e., concentration of zinc ion solution, carbonate solution concentration, flow rate of reagent addition and reactor temperature. Also, thermal decomposition study on the prepared zinc carbonate nanoparticles was carried out. Thermal analysis studies enable to monitor changes in weight and thermal events during the processes of dehydration and decomposition. These results were used for providing essential information on calcinations of $ZnCO_3$ precursor for its decomposition into single-dispersed nanometer crystalline ZnO.

To the best of our knowledge, although various reports could be found on the synthesis of zinc carbonate microparticles [13,14,16]; but, only a study on the synthesis of nanoparticles of $ZnCO_3$ precursor by grinding $ZnSO_4 \cdot 7H_2O$ and NH_4HCO_3 with surfactant OP thoroughly via the solid-state reaction at room temperature was reported [15] previously. Also, no information on the synthesis of basic zinc carbonate nanoparticles by the direct precipitation method has been reported in the literature. In this study, the precipitation and the thermal decomposition techniques were used for preparation of zinc carbonate and zinc oxide as two

simple, fast, and cost-effective methods; which have appropriate potential for scaling up for industrial scale production of the products. Meanwhile, in spite of previous studies in this investigation the products nanoparticles were prepared without any surfactant, template or catalyst.

2. Experimental

2.1. Materials and apparatus

Reagent-grade zinc nitrate, sodium carbonate and solvent (ethanol) were used as received from Merck. Scanning electron micrographs (SEM) were recorded on a Philips XL30 series instrument using a gold film for loading the dried particles on the instrument. Gold films were prepared by a Sputter Coater model SCD005 made by BAL-TEC (Switzerland). X-ray powder diffraction (XRD) was performed using a Rigaku D/max 2500V diffractometer equipped with a graphite monochromator and a Cu target. The IR spectra were measured on an IR spectrophotometer (Bruck Equinox 55) using the KBr pellet technique. Thermogravimetery (TG) and differential thermal analysis (DTA) were carried out using a Stanton Redcroft, STA-780 series with an aluminum crucible, applying heating rate of 10 °C min^{-1} in a temperature range of 50–600 °C, under nitrogen atmosphere with the flow rate of 50 ml min^{-1}. The sample mass used was about 3.0 mg. Transmission electron microscopic (TEM) image was obtained using a Ziess-EM900 scanning electron microscope. The sample preparation was carried out via coating on the Cu–carbon coated grid prior to the measurement.

2.2. $ZnCO_3$ synthesis and optimization strategy

$ZnCO_3$ particles were prepared by adding Zn^{2+} solution at various concentrations and different flow rates, to the carbonate solution under vigorous stirring and various reactor temperatures. After precipitation, the formed zinc carbonate was filtered and washed with distilled water three times. The product was then washed with ethanol two times and dried at 80 °C for 2 h. In order to optimize experimental parameters for the synthesis of $ZnCO_3$ nanoparticles, an experimental design approach was followed. The variables (zinc ion concentration, carbonate ion concentration, flow rate of feeding zinc reagent to the carbonate solution and reactor temperature) were as shown in Table 1.

2.3. Thermal decomposition synthesis of zinc oxide nanoparticles

Zinc oxide was obtained via thermal decomposition of the precursor. The $ZnCO_3$ sample, obtained by direct carbonation under optimum conditions, was used for calcinations process. The thermal decomposition synthesis of zinc oxide was carried out in a furnace at static air atmosphere at 700 °C for 2 h. 2 g of precursor was loaded without pressing into an open 30 mm diameter and 14 mm high alumina crucible.

3. Results and discussion

3.1. Results of synthesis by direct carbonation and optimization by OAD

Precipitation of a salt by mixing its anion and cation solutions is a commonly used technology for synthesis of various water insoluble inorganic materials such as $ZnCO_3$ [50]. The control of particle size and shape is a complex process requiring a fundamental comprehensation of the interactions of reagents. In this study, an attempt was made to determine how the various parameters of precipitation process affect the diameter of $ZnCO_3$ nanoparticles. Therefore, a Taguchi orthogonal array design [51–53] was used to identify the optimal conditions and to select the parameters having the most principal influence on the particle size and particle size distribution of zinc carbonate nanoparticles. Table 1 shows the structure of Taguchi's orthogonal array design and the results of measurements. The factors included in this study were zinc ion and carbonate solution concentrations, flow rate for addition of zinc solution to the carbonate solution and the temperature of the reactor. The scanning electron microscopic (SEM) images for the three samples of zinc carbonate obtained by this method are shown in Fig. 1. As shown in Table 1 the smallest values of particle size of zinc carbonate (33 nm) were obtained by

Table 1
OA_9 (3^4) experimental design and mean particle size of produced zinc carbonate as results.

Trial number	Zn^{2+} conc. (mol/L)	CO_3^{2-} conc. (mol/L)	CO_3^{2-} feed flow rate (ml/min)	Temperature (°C)	Diameter of $ZnCO_3$ particles (nm)
1	0.01	0.01	2.5	0	50
2	0.01	0.1	10	30	33
3	0.01	1.0	40	60	45
4	0.1	0.01	10	60	30
5	0.1	0.1	40	0	38
6	0.1	1.0	2.5	30	33
7	1.0	0.01	40	30	70
8	1.0	0.1	2.5	60	50
9	1.0	1.0	10	0	40

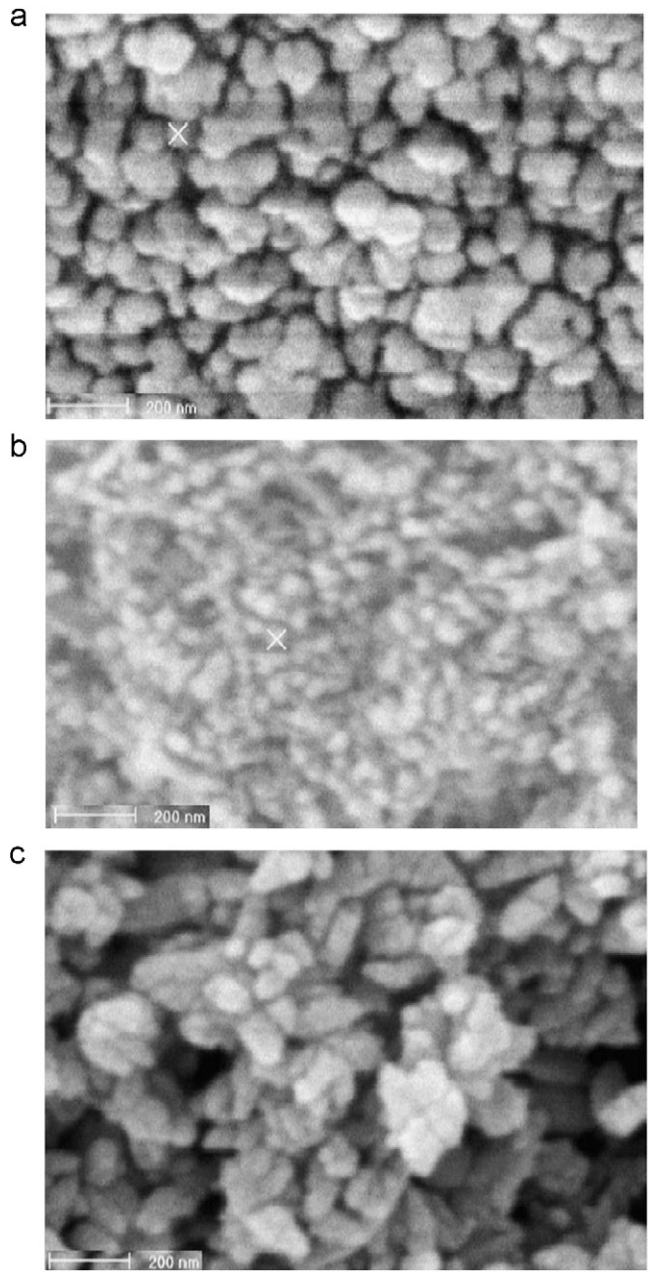

Fig. 1. SEM images of $ZnCO_3$ superstructures obtained at different runs, presented in Table 1, by direct carbonation according to experimental condition: (a) run 1, (b) run 2, and (c) run 3.

runs 2 and 6 while the largest values of particle size of product (70 nm) were produced in experimental run 7.

Since the experimental design is orthogonal, it is possible to separate the effect of each control factors at different levels by averaging responses at each level. The mean values of the particle size of the factors at each level were calculated according to assignment of the experiment (Table 2). In fact, computing of the average value of $ZnCO_3$ particle size corresponds to each factor, for example the effect of the carbonate solution concentration at level 1 (0.01 M) was carried out by pooling the particle size of produced $ZnCO_3$ among the nine trials in which

Table 2
Average particle size of $ZnCO_3$ for control factor and levels.

Factor	Level	Result (nm)
Zinc ion concentration (mol/L)	0.01	43
Zinc ion concentration (mol/L)	0.1	34
Zinc ion concentration (mol/L)	1.0	53
Carbonate ion concentration (mol/L)	0.01	50
Carbonate ion concentration (mol/L)	0.1	40
Carbonate ion concentration (mol/L)	1.0	39
Flow rate of zinc reagent (ml/min)	2.5	44
Flow rate of zinc reagent (ml/min)	10	34
Flow rate of zinc reagent (ml/min)	40	51
Temperature (°C)	0	43
Temperature (°C)	30	45
Temperature (°C)	60	42

Note: The results are diameter of zinc carbonate nano particles.

carbonate was set at level 1 (trials 1, 4 and 7) and dividing the result by the number of trials at this level (three). The average value for each level of any factor reveals how the particle size of produced $ZnCO_3$ will change when the level of the factor is varied.

The purpose of the analysis of variance (ANOVA) is to investigate which factors significantly affect the quality characteristic (which in this study was particle size of product, $ZnCO_3$). The analysis of data, when there is no interaction between variables, could determine the following results: (1) the optimum condition, (2) the individual influence of each factor at various levels, and (3) the particle size of zinc carbonate at the optimum condition. The results of analysis of variance (ANOVA) for the effect of various experimental parameters on the particle size of $ZnCO_3$ are shown in Table 3. In this table, S represents the sum of square of each variable or error term and V represents the variance of the results for each factor. The significance of the control factors on particle size characteristic can be estimated by the results of the ANOVA process. The significance means the extent of a control factor's effect on characteristics can be determined using the F values of the F-distribution. The F values are used to determine whether a control factor can be pooled to an error term or not. In general, the results of the experiments have a small degree of freedom, and therefore, a pooling method is used to increase the freedom of error.

In this study, the effect of zinc ion and carbonate ion concentrations on the particle size of synthesized zinc carbonate at three different levels (0.01, 0.1 and 1.0 mol/L) was investigated. It was found that concentrations of zinc ion and carbonate solution are significant parameters for controlling the particle size of $ZnCO_3$ product. Also, the effect of flow rate corresponding to addition of zinc reagent into the reactor on the size of $ZnCO_3$ particles was studied. Three different flow rates (2.5, 10 and 40 ml/min) were investigated. Our finding showed that flow rate is a significant parameter for controlling paticle size of $ZnCO_3$. Another investigated parameter for controlling the particle size of zinc carbonate was temperature of the reactor. The

Table 3
Results of ANOVA for $ZnCO_3$ nanoparticles synthesis using direct carbonation procedure by OA_9 (3^4) matrix.

Factor	Code	DOF	S	V	DOF	S' pooled	F	P' (%)[a]
Zinc concentration (mol/L)	C_{Zn}	2	581.5	290.8	2	538.5	27.0	43.65
Carbonate concentration (mol/L)	C_{CO_3}	2	208.2	104.1	2	165.2	9.7	13.39
Flow rate (ml/min)	F	2	422.2	211.1	2	379.2	19.6	30.74
Temperature (°C)	T	2	21.5	10.7	–	–	–	–
Error	–	–	–	–	2	21.5	–	12.22

Note: The critical value was at 90% confidence level; pooled error results from pooling of insignificant effect.
[a]Percentage of contribution.

results showed that temperature is not a significant parameter for the control of $ZnCO_3$ paticle size.

The ANOVA results of these experiments indicate that (at 90% confidence level) except temperature, all other variables (zinc and carbonate concentrations and flow rate) have significant effects on the particle size of zinc carbonate. In this work, the interactions between the varibles were not considered. The results of ANOVA indicated that 0.1 mol/L is the optimum zinc concentration for generation of $ZnCO_3$ nanoparticles. Also, by increasing carbonate concentration from 0.01 to 1.0 mol/L, the particle size of $ZnCO_3$ particles was decreased. Therefore, 1.0 mol/L was selected as optimum concentration of carbonate ion. On the other hand, 10 mL/min flow rate for addition of zinc ion to the carbonate solution is the optimum flow rate for generation of $ZnCO_3$ nanoparticles.

Under the optimized levels of the significant factors, obtained from the OA_9 (3^4) matrix (Table 3), the performance of the procedure (particle size of zinc carbonate) could be calculated according to the following expression:

$$Y_{opt} = \frac{T}{N} + \left(C_{Zn} - \frac{T}{N}\right) + \left(C_{CO_3} - \frac{T}{N}\right) + \left(F_{Zn} - \frac{T}{N}\right)$$

where T/N is the average size of $ZnCO_3$ particles obtained from nine experimental runs+contribution of C_{Zn}, C_{co_3} and F_{Zn} above average performance; while, T is the grand total of all results for particle size, N is the total number of results, Y_{opt} is the diameter of nanoparticles under optimum condition, C_{Zn}, C_{CO_3} and F_{Zn} are the average particle size of the product at optimum levels of zinc and carbonate solution concentrations and flow rate, respectively. On the other hand, under optimum conditions, the confidence interval (CI) for the particle size of zinc carbonate is calculated using the following expression:

$$CI = \pm\sqrt{\frac{F_\alpha(f_1,f_2)V_e}{N_e}}$$

where $F_\alpha(f_1,f_2)$ is the F value from the F table at the degrees of freedom (DOF), f_1 and f_2 at the level of significance α (in this work, α=90%), $f_1=DOF$ of mean (which always equals 1), $f_2=DOF$ of the pooled error term, N_e=effective number of replications, and given by N_e=number of trials/(DOF of mean (always equals 1)+total DOF of factors used for the prediction). Calculations for prediction of the particle size of product at optimum condition and CI for this estimated particle size showed that with a 90% confidence level under optimum conditons, the size of $ZnCO_3$ particles will be 20 ± 6 nm.

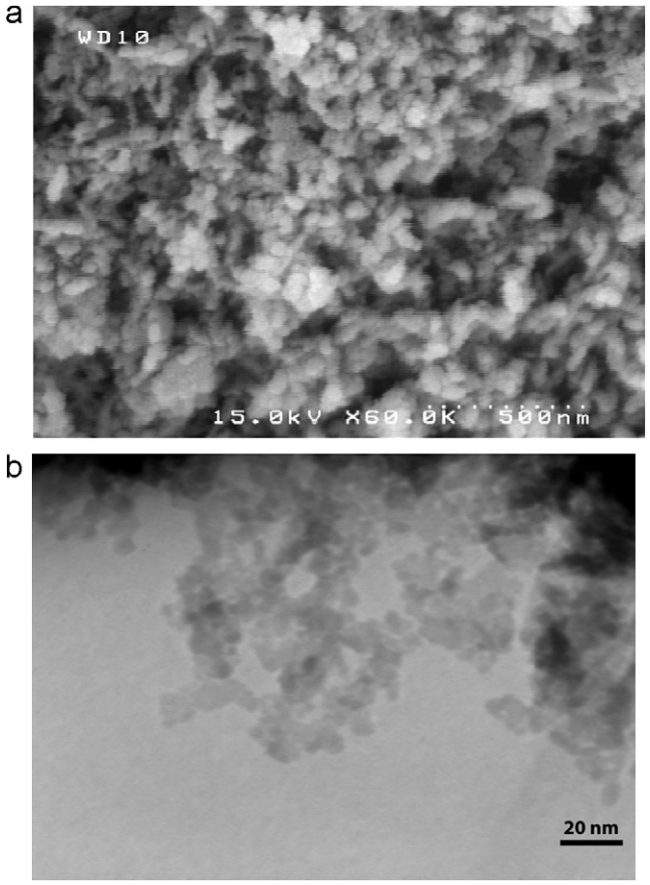

Fig. 2. (a) SEM image and (b) TEM image of $ZnCO_3$ nanoparticles obtained under optimum conditions by direct carbonation.

3.2. Characterization of zinc carbonate nanoparticles prepared under optimum condition

In the next step of this investigation, zinc carbonate nanoparticles were prepared under optimum condition obtained from the results of ANOVA (0.1 mol/L concentration of zinc ion, 1.0 mol/L concentration of carbonate ion and 10 mL/min flow rate for addition of zinc ion

reagent to the carbonate solution). The results of SEM revealed that the prepared zinc carbonate particles under optimum condition have about 15 nm average diameter (Fig. 2a). Also, TEM image of zinc carbonate nanoparticles prepared under optimum conditions (Fig. 2b) confirms the SEM result. The as-prepared zinc carbonate sample at this condition was used for XRD, FT-IR and thermal analysis studies.

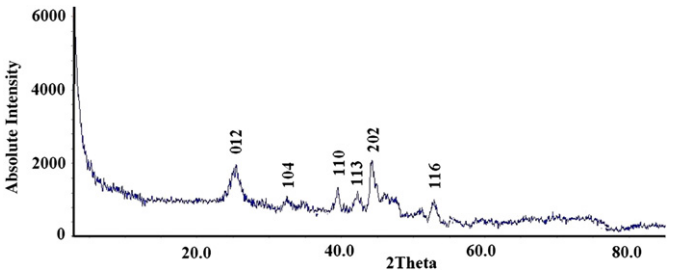

Fig. 3. XRD pattern of the zinc carbonate prepared by direct precipitation from reagents solution under optimum conditions.

Fig. 3 shows the XRD pattern of the zinc carbonate nanoparticles obtained under optimum condition. Most of the diffraction peaks in the figure can be indexed to be in agreement with the trigonal system structure of $ZnCO_3$ from PDF card 83-1765. However, the moderate intensity and non-smoothed baseline and a wide and low diffraction spectrum of the as-prepared $ZnCO_3$ indicated that the precursor was more in amorphous form and has a lower degree of crystallinity. Meanwhile, some other small peaks observed in the XRD pattern are corresponding to the presence of hydroxyl groups in the product [54].

In addition, the spectral nature of the as-prepared zinc carbonate shows a broad band in the near-IR region, which is the characteristic band for zinc carbonate [54]. The fourier transform infrared (FT-IR) spectrum of the produced spherical-shaped zinc carbonate nanoparticles at

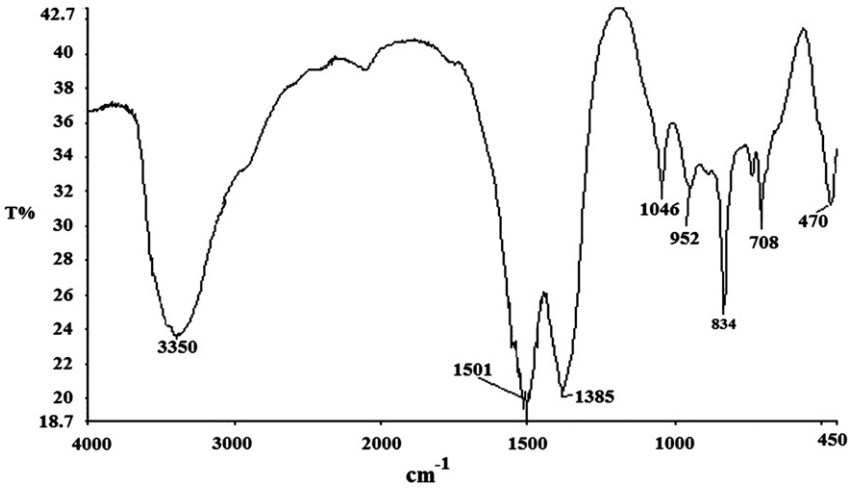

Fig. 4. FT-IR spectra of the precipitated zinc carbonate nanoparticles obtained under optimum conditions.

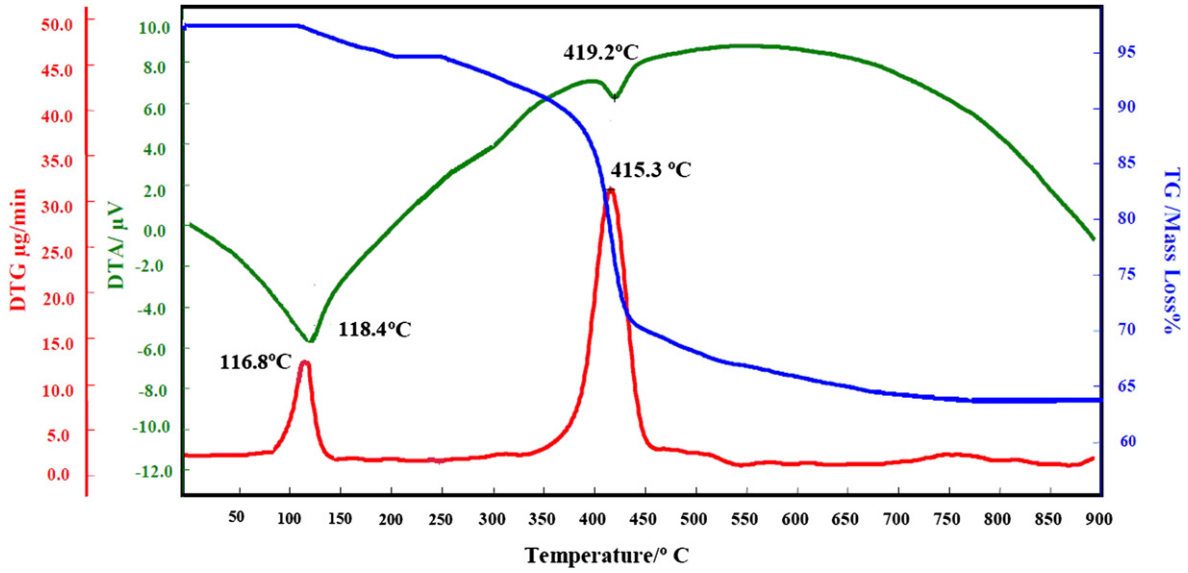

Fig. 5. TG/DTG/DTA curves for thermal decomposition reaction of $ZnCO_3$ precursor; sample mass 3.0 mg, heating rate 10 °C min^{-1}, and nitrogen atmosphere.

the optimum condition is shown in Fig. 4. The presence of peaks in IR spectrum at 700–1100 cm^{-1} are related to carbonate ion and shows the formation of zinc carbonate [55]. Also, it can be seen that, the absorption peak in 3380–3600 cm^{-1} is stretching vibration of hydrogen bond, indicating the plentiful existence of hydroxyl group and formation of zinc carbonate in the basic form. The peaks at 1384 cm^{-1} and 1625 cm^{-1} are attached to $ZnCO_3$, and the absorption tape in 700–1100 cm^{-1} are due to the lattice vibration of CO_3^{2-} [56].

The thermoanalytical graphs of zinc carbonates nanoparticles parepared under optimum experimental conditions are presented in Fig. 5. The TG–DTG–DTA results, obtained under nitrogen atmosphere, show the precursor losses its weight during two steps. The first step is in the temperature range of 100–160 °C, indicating the dehydration of surface-adsorbed water. The second step is a major weight loss tape in the temperature range of 260–500 °C, indicating the loss of OH^- and CO_3^{2-} from basic zinc carbonate particles. The mass-loss due to the thermal decomposition of basic zinc carbonate observed by TG, 26.4% in the temperature range of 260–500 °C, corresponds to assuming the following reaction (with the theoretical value of 25.9%) [57]:

$$Zn_5(CO_3)_2(OH)_6 \rightarrow 5ZnO + 2CO_2 + 3H_2O$$

Thermal decomposition of the precursor was basically complete at 700 °C, which indicates that the optimum calcination temperature is 700 °C. The DTA curve shows an obvious endothermic peak around 419 °C, which illustrates that the decomposition of OH^- and CO_3^{2-} happens simultaneously. The weight of the carbonate sample after 700 °C was kept approximately constant, which indicated that the precursor had been entirely decomposed into ZnO. After moisture loss by the sample, except for a strong endothermic peak at 419.2 °C, there was no other absorption peak before the constant weight on the DTA curve. It indicated that the precursor only had a single decomposition step.

3.3. ZnO nanoparticles preparation by calcination of basic zinc carbonate

By using the results of TG–DTA for basic zinc carbonate nanoparticles, obtained by direct precepiation under the optimum conditions, zinc oxide nanoparticles were prepared via thermal decomposition of the precursor at 700 °C. The scanning electron microscopic (SEM) image for the prepared sample of zinc oxide by this method is shown in Fig. 6a. The average particle size of zinc oxide produced by calcinations of the precursor was about 20 nm. This result is cofirmed by TEM image of ZnO prepared under optimum conditions (Fig. 6b).

Also, Fig. 7 shows the XRD pattern of the zinc oxide nanoparticles obtained via thermal decomposition of precursor. Strong intensity, smoothed baseline and a wide and low diffraction in spectrum of the produced zinc oxide were observed. This indicated that the zinc oxide produced by calcinations of the precursor is crystalline with high purity. All the diffraction peaks in the figure can be indexed to be in agreement with the hexagonal system structure of ZnO from PDF card 89-1397.

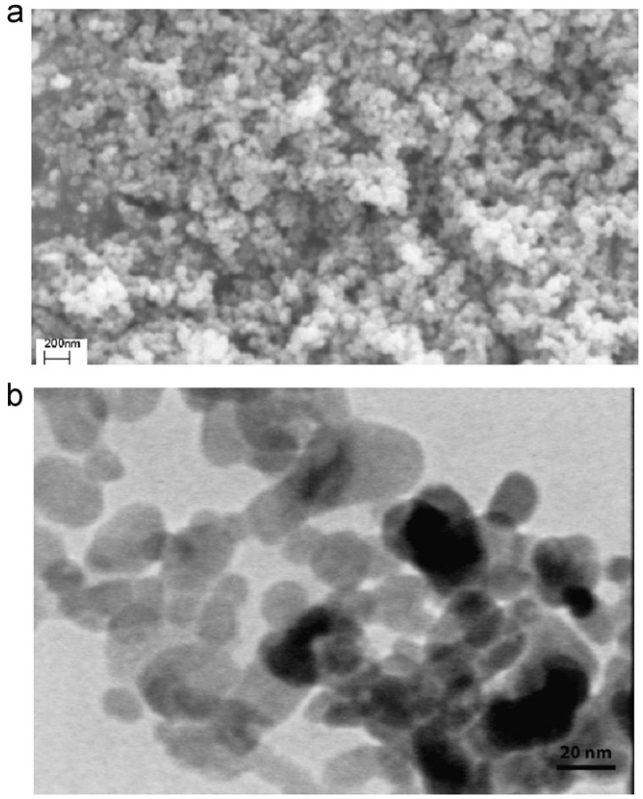

Fig. 6. (a) SEM image and (b) TEM image of ZnO nanoparticles obtained from thermal decomposition reaction of precursor.

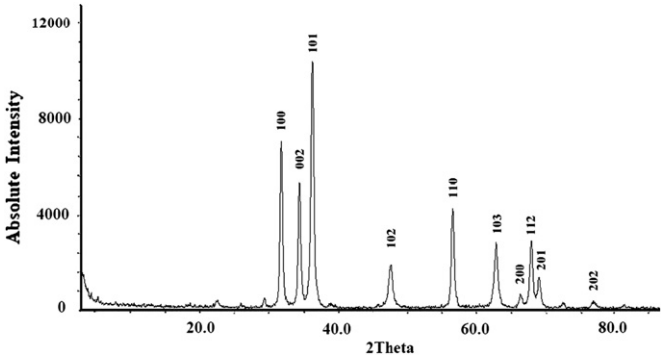

Fig. 7. XRD pattern of zinc oxide prepared by thermal decomposition reaction of precursor.

Fig. 8 shows the infrared (IR) spectrum of the ZnO sample prepared by calcination of the precursor at 700 °C for 2 h. The results are coincident with Refs. [58,59] and show the formation of highly pure zinc oxide. In comparison with IR spectrum of precursor (Fig. 4), it can be seen that the absorption peak in 3380–3600 cm^{-1} which arises from the stretching vibration of hydrogen bond due to the

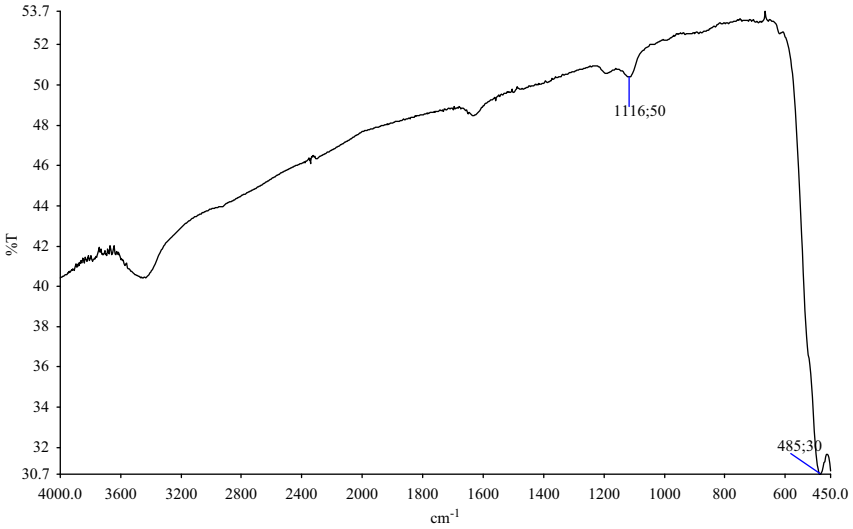

Fig. 8. FT-IR spectra of the zinc oxide nanoparticles obtained by thermal decomposition reaction of precursor.

plentiful existence of hydroxyl group in precursor has been reduced significantly in Fig. 8, illustrating the complete decomposition of hydroxyl group after calcination of the precursor. In Fig. 8, the sharp peaks between 700 and 1000 cm^{-1} weaken greatly only leaving some weak fluctuation peaks. It is obvious that the two peaks at 1383 cm^{-1} and 1505 cm^{-1} become very weak and split into three absorption peaks. Also, three peaks around 700–1100 cm^{-1} weaken with the decomposition of zinc hydroxy carbonate, indicating the decomposition of carbonate.

4. Conclusion

A facile precipitation reaction method was proposed for preparation of basic zinc carbonate nanoparticles. The precipitation technique is a controllable method for the synthesis of $ZnCO_3$ nanoparticles in the aqueous media at low temperature. The Taguchi robust design was used to optimize the reaction parameters for obtaining desired particle size. The result showed that zinc ion concentration, carbonate solution concentration, and flow rate of zinc reagent addition to the carbonate ion solution having significant effects on particle size of the produced zinc carbonate. Basic zinc carbonate nanoparticles were prepared under optimal condition with about 15 nm diameter. Thermal analysis studies showed that zinc carbonate decomposes via a single stage process to zinc oxide. The average particle diameter of ZnO prepared by calcinations of the precursor was about 20 nm which was comparable than that of $ZnCO_3$ precursor. The presented methods for preparation of zinc carbonate and zinc oxide nanoparticles have many advantages, such as simplicity, low cost, high output and little pollution in addition to superfine compounds that can be easily prepared in relatively large scales.

References

[1] Z. Deng, S. Xu, S. Li, International Journal of Pharmacology 351 (2008) 236–243.
[2] S.M. Pourmortazavi, S.S. Hajimirsadeghi, Industrial and Engineering Chemistry Research 44 (2005) 6523–6533.
[3] W.B. Ko, J.M. Yun, S.W. Jo, Y.S. Shon, Ultrasonics 44 (2006) e363–e366.
[4] M. Shamsipur, S.M. Pourmortazavi, M. Roushani, I. Kohsari, S.S. Hajimirsadeghi, Microchimica Acta 173 (2011) 445–451.
[5] S.M. Pourmortazavi, I. Kohsari, S.S. Hajimirsadeghi, Central European Journal of Chemistry **7** (2009) 74–78.
[6] S. Zhang, H. Fortier, J.R. Dahn, Materials Research Bulletin 39 (2004) 1939.
[7] M.J. Abler, US Patent 5344626, 1994.
[8] X. Feng, Z. Li, P. Wang, Y. Zhou, Journal of Materials Science 40 (2005) 6597–6600.
[9] S. Kaluza, M. Muhler, Catalysis Letters 129 (2009) 287–292.
[10] P. Kuai, C. Liu, P. Huo, Catalysis Letters 129 (2009) 493–498.
[11] Q.W. Li, G.A. Luo, Y.Q. Shu, Analytica Chimica Acta 2 (2000) 137–142.
[12] K. Kakiuchi, E. Hosono, T. Kimura, H. Imai, S. Fujihara, Journal of Sol–Gel Science and Technology 39 (2006) 63–72.
[13] S. Zhang, H. Fortier, J.R. Dahn, Materials Research Bulletin 39 (2004) 1939–1948.
[14] Y.B. Feng, W.Q. Lu, J.Y. Cao, Z. Cai, P.F. Wang, Chinese Journal of Inorganic Chemistry 4 (2003) 428–432.
[15] W. Wu, Q. Jiang, Materials Letters 60 (2006) 2791–2794.
[16] S.M. Pourmortazavi, S.S. Hajimirsadeghi, M. Rahimi-Nasrabadi, Journal of Dispersion Science and Technology 33 (2012) 254–257.
[17] S.M. Pourmortazavi, S.S. Hajimirsadeghi, M. Rahimi-Nasrabadi, I. Kohsari, Chemical Engineering Communications 198 (2011) 1182–1188.
[18] M. Schur, B. Bems, A. Dassenoy, I. Kassatkine, J. Urban, H. Wilmer, O. Hinrichsen, M. Muhler, R. Schlogl, Angewandte Chemie International Edition 42 (2003) 3815.
[19] M. Salavati-Niasari, N. Mir, F. Davar, Journal of Alloys and Compounds 493 (2010) 163–168.
[20] F. Davar, M. Salavati-Niasari, Z. Fereshteh, Journal of Alloys and Compounds 496 (2010) 638–643.
[21] M. Salavati-Niasari, F. Davar, A. Khansari, Journal of Alloys and Compounds 509 (2011) 61–65.

[22] M. Salavati-Niasari, N. Mir, F. Davar, Journal of Alloys and Compounds 493 (2010) 163–168.
[23] F. Mohandes, F. Davar, M. Salavati-Niasari, Journal of Magnetism and Magnetic Materials 322 (2010) 872–877.
[24] M. Salavati-Niasari, F. Davar, Z. Fereshteh, Journal of Alloys and Compounds 494 (2010) 410–414.
[25] M. Salavati-Niasari, A. Sobhani, F. Davar, Journal of Alloys and Compounds 507 (2010) 77–83.
[26] Z. Ji, S. Zhao, C. Wang, K. Liu, Materials Science and Engineering B 117 (2005) 63–66.
[27] K. Suzuki, M. Inoguchi, K. Kageyama, H. Takagi, Y. Sakabe, Journal of Nanoparticle Research 11 (2009) 1349–1360.
[28] X. Cao, N. Wang, L. Wang, L. Guo, Journal of Nanoparticle Research 12 (2010) 143–150.
[29] M. Copuroglu, L.H.K. Koh, S. O'Brien, G.M. Crean, Journal of Sol–Gel Science and Technology 52 (2009) 432–438.
[30] D.N. Kanari, D. Mishra, I. Gaballah, B. Dupre, Thermochimica Acta 410 (2004) 93.
[31] N. Koga, J.M. Criado, H. Tanaka, Journal of Thermal Analysis and Calorimetry 60 (2000) 943.
[32] G. Pfaff, in: R. Dittmeyer, W. Keim, G. Kreysa, A. Oberholz (Eds.), ChemTech, vol. 7, Wiley-VCH, Weinheim, 2005.
[33] Zs. Ehen, Cs. Novak, J. Sztatisz, O. Bene, Journal of Thermal Analysis and Calorimetry 78 (2004) 427.
[34] N. Koga, H. Tanaka, Thermochimica Acta 388 (2002) 41.
[35] B. Donkova, D. Mehandjiev, Journal of Materials Science 40 (2005) 3881–3886.
[36] Y. Murata, S. Fukuta, S. Ishikawa, S. Yokoyama, Solar Energy Materials and Solar Cells 62 (2000) 157.
[37] T. Alammar, A.V. Mudring, Journal of Materials Science 44 (2009) 3218–3222.
[38] S.D. Jones, L.M. Neal, H.E. Hagelin-Weaver, Applied Catalysis B—Environmental 84 (2008) 631–642.
[39] H.M. Deng, J. Ding, Y. Shi, X.Y. Liu, J. Wang, Journal of Materials Science 36 (2001) 3273–3276.
[40] L. Goris, R. Noriega, M. Donovan, J. Jokisaari, G. Kusinski, A. Salleo, Journal of Electronic Materials 38 (2009) 586–595.
[41] J. Liqiang, W. Baiqi, X. Baifu, L. Shudan, S. Keying, C. Weimin, F. Honggang, Journal of Solid State Chemistry 177 (2004) 4221–4227.
[42] C.C. Li, Z.F. Du, L.M. Li, H.C. Yu, Q. Wan, T.H. Wang, Applied Physics Letters 91 (2007) 101.
[43] S. Liang, H. Sheng, Y. Liu, Z. Hio, Y. Lu, H. Shen, Journal of Crystal Growth 225 (2001) 553.
[44] Z.L. Wang, Journal of Physics: Condensed Matter 16 (2004) R829.
[45] G. Hengxiang, H. Yunyao, W. Qifeng, J. Guojuan, F. Zebo, W. Yinyue, Semiconductor Photonics and Technology 10 (2004) 97–100.
[46] Z. Xitang, Z. Jiaqi, X. Jinjie, X. Tengfeng, W. Dejun, B. Yubai, L. Tiejin, Y. Jiannian, Chemical Journal of Chinese Universities 20 (1999) 1945–1947.
[47] D. Banerjee, J. Rybczynski, J.Y. Huang, D.Z. Wang, K. Kempa, Z.F. Ren, Applied Physics A 80 (2005) 749.
[48] A.C. Mofor, A. Bakin, A. Elshaer, D. Fuhrmann, F. Bertram, A. Hangleiter, J. Christen, A. Waag, Physica Status Solidi C3 (2006) 1046.
[49] M. Lorenz, E.M. Kaidashev, A. Rahm, T. Nobis, J. Lenzner, G. Wagner, D. Spemann, H. Hochmuth, M. Grundmann, Applied Physics Letters 86 (2005) 113.
[50] S.M. Pourmortazavi, S.S. Hajimirsadeghi, I. Kohsari, R. Fareghi Alamdari, M. Rahimi-Nasrabadi, Chemical Engineering and Technology 31 (2008) 1532–1535.
[51] G. Taguchi, Systems of Experimental Design, vol. 1–2, Kraus, New York, 1987.
[52] R.K. Roy, A Primer on the Taguchi Method, New York, Van Nostrand Reinhold, 1990.
[53] S.M. Pourmortazavi, S.S. Hajimirsadeghi, I. Kohsari, S.G. Hosseini, Journal of Chemical and Engineering Data 49 (2004) 1530–1534.
[54] Z. Xianxi, W. Xiaojuan, Z. Guanjie, J. Jianzhuang, Chinese Journal of Inorganic Chemistry 18 (2002) 1038–1040.
[55] D. Stoilova, V. Koleva, V. Vassileva, Spectrochimica Acta Part A 58 (2002) 2051.
[56] H. Yongning, S. Xiaoliang, M. Lidun, Chinese Journal of Applied Chemistry 13 (1996) 92–94.
[57] N. Koga, H. Tanaka, Journal of Thermal Analysis and Calorimetry 82 (2005) 725–729.
[58] Liu Chao-feng, Hu Xing-fang, Zu Yong, Nanometer sized zinc oxide prepared by using urea as precipitating agent [J], Journal of Inorganic Materials 14 (3) (1999) 391–396 (in Chinese).
[59] W. Wu, Y.W. Cai, J.F. Chen, S.L. Shen, A. Martin, L.-X. Wen, Journal of Materials Science 41 (2006) 5845–5850.